Journal of Asian Earth Sciences 114 (2015) 352–361

Contents lists available at ScienceDirect

Journal of Asian Earth Sciences

journal homepage: www.elsevier.com/locate/jseaes

Multiple seismo-anomalies associated with the M6.1 Ludian earthquake on August 3, 2014

Xiaoping Zeng [a], Yunfang Lin [a], Weisheng Chen [b], Zhiqiang Bai [b], Jann-Yenq Liu [c,d], Chieh-Hung Chen [e,*]

[a] Institute of Geophysics, China Earthquake Administration, Beijing 100081, China
[b] Institute of Earthquake Prediction, Beijing University of Technology, Beijing 100124, China
[c] Institute of Space Science, National Central University, Jhongli 320, Taiwan
[d] Center for Space and Remote Sensing Research, National Central University, Jhongli 320, Taiwan
[e] Department of Earth and Environmental Sciences, National Chung Cheng University, Chiayi 621, Taiwan

ARTICLE INFO

Article history:
Received 31 August 2014
Received in revised form 12 March 2015
Accepted 16 April 2015
Available online 30 April 2015

Keywords:
Groundwater
Water temperature
Radon
Electromagnetic field
Total electron content
Earthquake forecast

ABSTRACT

Multiple geophysical parameters including groundwater level, water temperature, water radon, crustal deformation, electromagnetic waves and total electron contents (TEC) in the ionosphere, are examined together to investigate pre-earthquake anomalous phenomena associated with the Mw6.1 Ludian earthquake on August 3, 2014. Cross-parameter comparison eliminates anomalies that are detected in one parameter only and examine earthquake-related phenomena in various fields, simultaneously. Retrieved anomalies show that abnormal decreases of water temperature and radon concentration related to anomalous uplift of groundwater levels appeared about 1–8 days before the earthquake even without contributions from rain. Significant step-like changes are observed from data recorded by strainmeters on July 31 and are consistent with water-related anomalies in timing. No significant anomalies can be found from electromagnetic data through the preliminary observation. In contrast, TEC appeared positive anomalies 1–3 days before the Ludian earthquake. Although causal mechanisms of the TEC anomalies from stressed rocks are not fully understood, multiple-parameter examination can increase credibility of determination regarding pre-earthquake phenomena.

1. Introduction

The Yunnan area is located in the southern part of China and the northeastern margin of the convergent plate boundary between the Indian and Eurasian plates. Intense interactions between the Indian and Eurasian plates formed complex tectonic structures and many earthquakes. On August 3, 2014, an earthquake (103.4°E, 27.2°N) with magnitude (Mw) of 6.1 and 10 km in depth struck south China with its epicenter near the Ludian County, Yunnan at 16:30:10 (local time). The earthquake caused loss of 617 lives, missing of 112 people and collapse of more than 80,000 buildings. About 230 thousand of people were promptly evacuated from disaster areas and arranged to safe places. The total number of approximately 1 million people was disaster-stricken during the Ludian earthquake. The centroid moment tensor analysis indicates that the Ludian earthquake was caused by the strike-slip fault, with the strike 70°, dip 85°, and rake 180° (http://www.globalcmt.org/). The most compressive axis of the earthquake is about 294° by using the standard method proposed by Robinson and McGinty (2000). The Ludian-Zhaotong fracture zone with a north–south strike is located at the eastern side and very close to the epicenter. Meanwhile, its aftershocks aligned in an east–west trend along the Xiaojiang-Baogunao fracture zone. Those two fracture zones with the approximately perpendicular relationship of the strikes would dominate the strike-slip fault triggering the Ludian earthquake.

Many previous studies (Scholz et al., 1973; Molchanov and Hayakawa, 2008; Freund, 2013) reported that information about pre-earthquake anomalous phenomena can be extracted from routinely recorded data of several physical parameters. The causal mechanism of earthquakes is resulted from stress accumulating in the crust. To monitor earthquake-related stress via strain, data recorded by ground-based GPS (Global Positioning System) stations (Peltzer et al., 1998; Barbot et al., 2008; Barbot and Fialko, 2010; Chen et al., 2011, 2013a, 2014, 2015) and/or strainmeters (Smith and Gomberg, 2009) are often utilized. Anomalous uplift and depression of groundwater levels are often observed prior to earthquakes while the permeability of rocks would be modified by loading stress (Bredehoeft, 1967; Chia et al., 2001; Kingsley

* Corresponding author. Tel.: +886 5 2720411x66200.
E-mail address: nononochchen@gmail.com (C.-H. Chen).

http://dx.doi.org/10.1016/j.jseaes.2015.04.027
1367-9120/

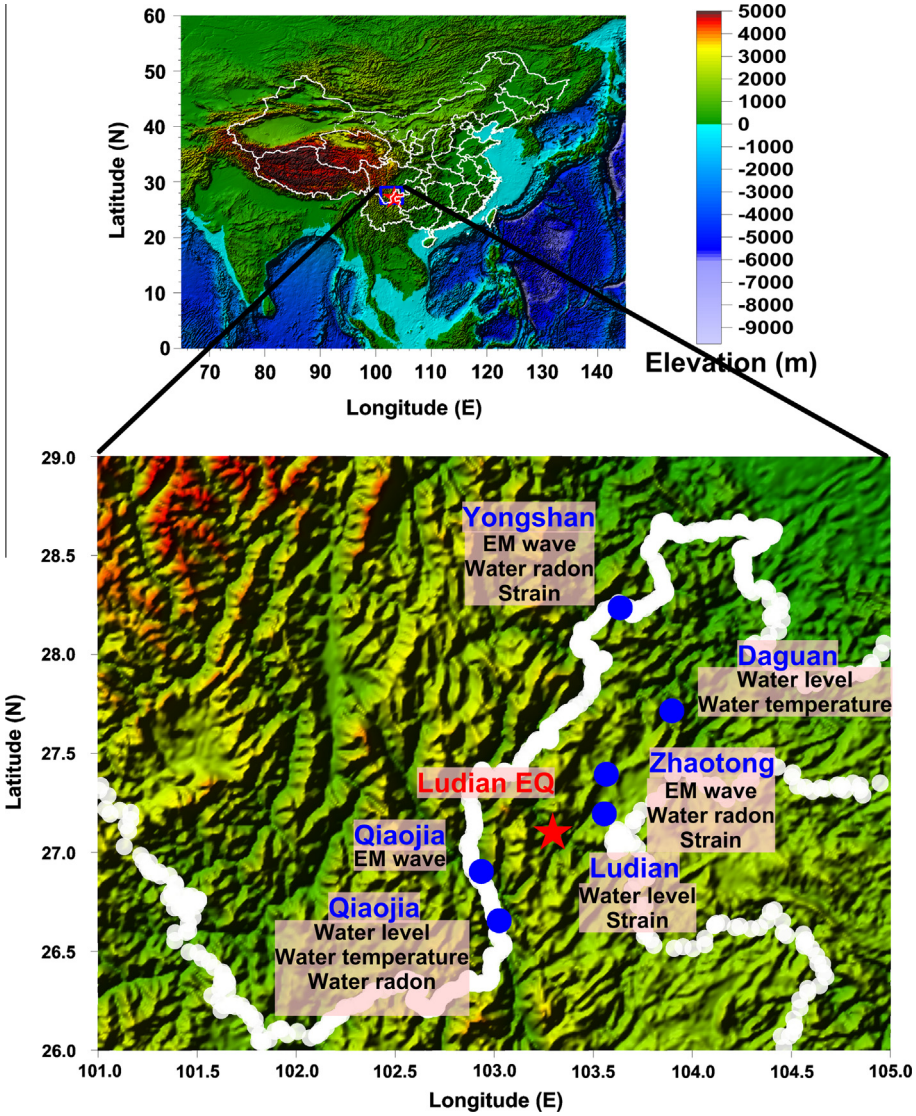

Fig. 1. Locations of the epicenter of the Ludian earthquake and utilized stations lies on the topography map. The red star denotes the location of the epicenter. The blue circles show stations. (For interpretation of the references to color in this figure legend, the reader is referred to the web version of this article.)

et al., 2001; Quilty and Roeloffs, 1997; Roeloffs, 1988, 1998; Wang et al., 2001; Chen et al., 2013b). Meanwhile, earthquake-related stress can open and/or close of ducts, in which gas could propagate from deep depth to shallow subsurface, owing to developments of cracks (Scholz et al., 1973). Gases from deep depth would partially dissolve in groundwater to modify the associated concentration. Thus, a change in concentration, particularly for groundwater radon, is generally considered to be one of the promising candidates of pre-earthquake anomalous phenomena to monitor seismic activity (Wakita et al., 1980; Kuo et al., 2006; Ghosh et al., 2009).

Stress accumulation in the crust can simultaneously change conductivity (Lin and Zeng, 1992; Zeng et al., 1995) and/or susceptibility (Stacey, 1962; Nagata, 1970) underground and yield electric currents (Merzer and Klemperer, 1997; Yen et al., 2004) to change electromagnetic field (Fraser-Smith et al., 1990; Hattori, 2004; Hattori et al., 2013; Liu et al., 2006; Molchanov and Hayakawa, 2008; Chen et al., 2009, 2010, 2013c; Han et al., 2009, 2011, 2014, 2015; Wen et al., 2012; Xu et al., 2013) that are believed to be due to electrokinetic (Fenoglio et al., 1995), microfracturing (Molchanov and Hayakawa, 1995), piezoelectric effects (Huang, 2002) and activation of positive holes (Freund et al., 2006; Freund, 2010, 2013). These studies have shown that seismo-electromagnetic anomalies distribute within a wide frequency band from direct current (DC) to very low frequency (VLF). Meanwhile, seismo-electromagnetic anomalies are one of potential parameters to affect electric field near and/or above the Earth's surface and further change the total electron contents (TEC) in the ionosphere (Kuo et al., 2011). The global ionosphere map (GIM) of TEC constructed with about 200 of worldwide ground-based receivers of the GPS is routinely published in a 2-h time interval (ftp://cddisa.gsfc.nasa.gov/pub/gps/products/ionex). The GIM reveals that TECs with significantly anomalies over the epicenter a few days before the 12 May 2008 M8.0 Wenchuan earthquake, the 26 December 2004 M9.3 Sumatra–Andaman earthquake, and the 12 January 2010 M7.0 Haiti earthquake (Liu et al., 2009, 2010, 2011). Liu et al. (2009) statistically examined the GIM TECs over 35 $M \geqslant 6.0$ earthquakes occurring in China during the 10-year period of May 1, 1998–April 30, 2008, and often found pronounced decrease anomalies of the TEC over the epicenter on day 3–5 before 17 $M \geqslant 6.3$ earthquakes.

Here, ground-station data of strain, groundwater level, water temperature, water radon and electromagnetic field, monitored

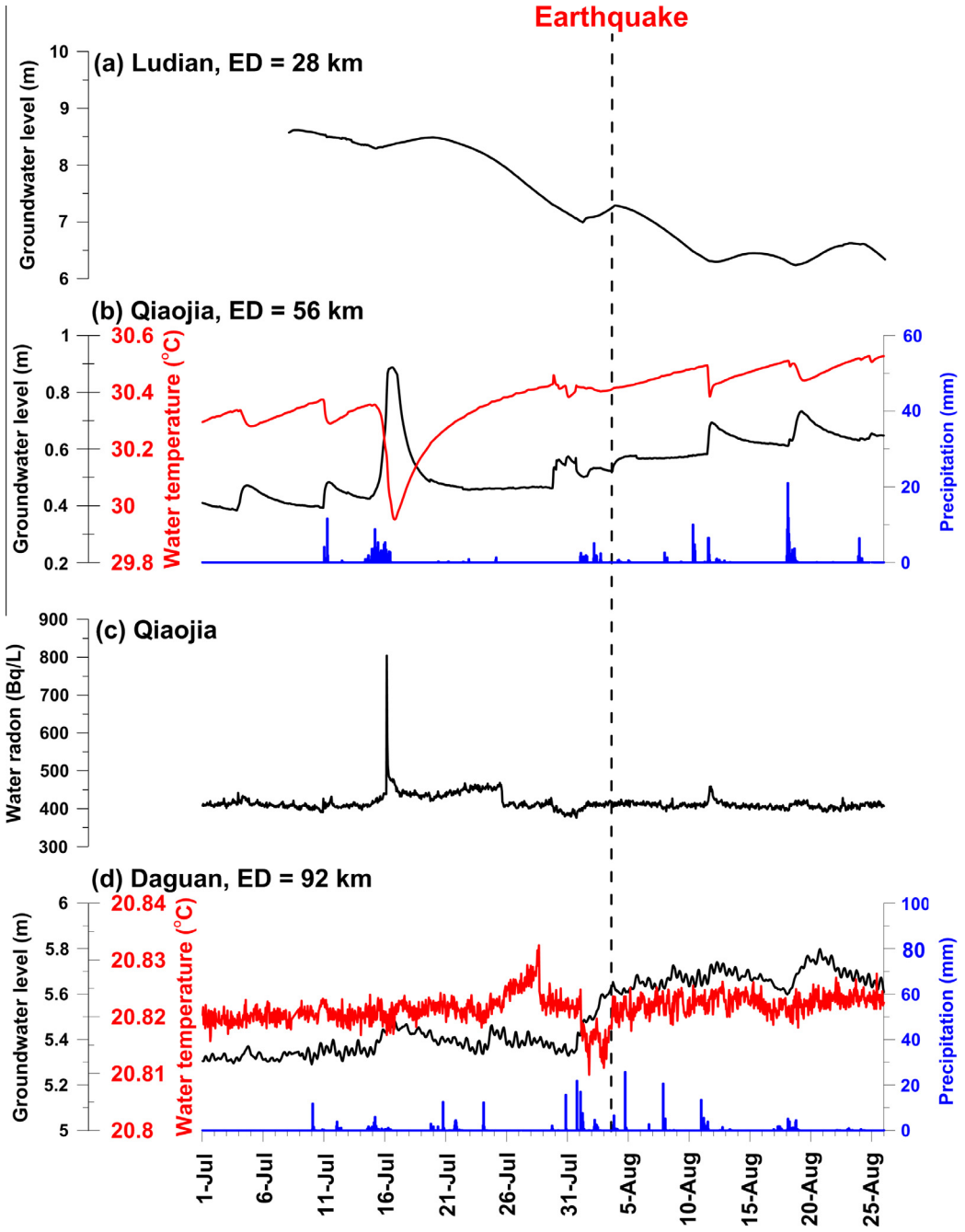

Fig. 2. Variations of groundwater level, water temperature, water radon and precipitation in Ludian, Qiaojia and Daguan during July 1–August 25. The vertical dash line shows occurrence time of the Ludian earthquake. The data and the accordingly *Y* axis is paired by the same color. ED is the abbreviation of epicentral distance. (For interpretation of the references to color in this figure legend, the reader is referred to the web version of this article.)

by instruments at Daguan, Ludian, Qiaojia, Yongshan and Zhaotong (also see Fig. 1), covering the period from July 1 to August 15, 2014, are utilized to report anomalous phenomena associated with the Ludian earthquake. Meanwhile, the TEC in the ionosphere over the epicenter retrieved from GIM during July 14–August 14, 2014 is accordingly examined to achieve the lithosphere–atmosphere–ionosphere coupling. The data retrieved during this period are compared with time-series data from normal periods and processed to identify earthquake-related anomalous phenomena. The determined time-dependent anomalous phenomena from entire physical parameters are integrated together to cross-check their relationships via potential physical mechanisms.

2. Observations of groundwater level, water temperature, precipitation and radon

Hourly changes in groundwater level, water temperature and radon at Ludian, Qiaojia and Daguan from July 1 to August 25 are shown in Fig. 2. A decreasing trend can be found from groundwater level at the Ludian station during the study period (Fig. 2a). Uplift changes, which lay on the decreasing trend, can be observed on July 16, August 1, August 12 and August 19 in 2014. Those smooth uplifts were most likely resulted from rainfalls, except for it on August 1, when the precipitation recorded at the Qiaojia station is also taken into account. Notably, the sudden change, which is

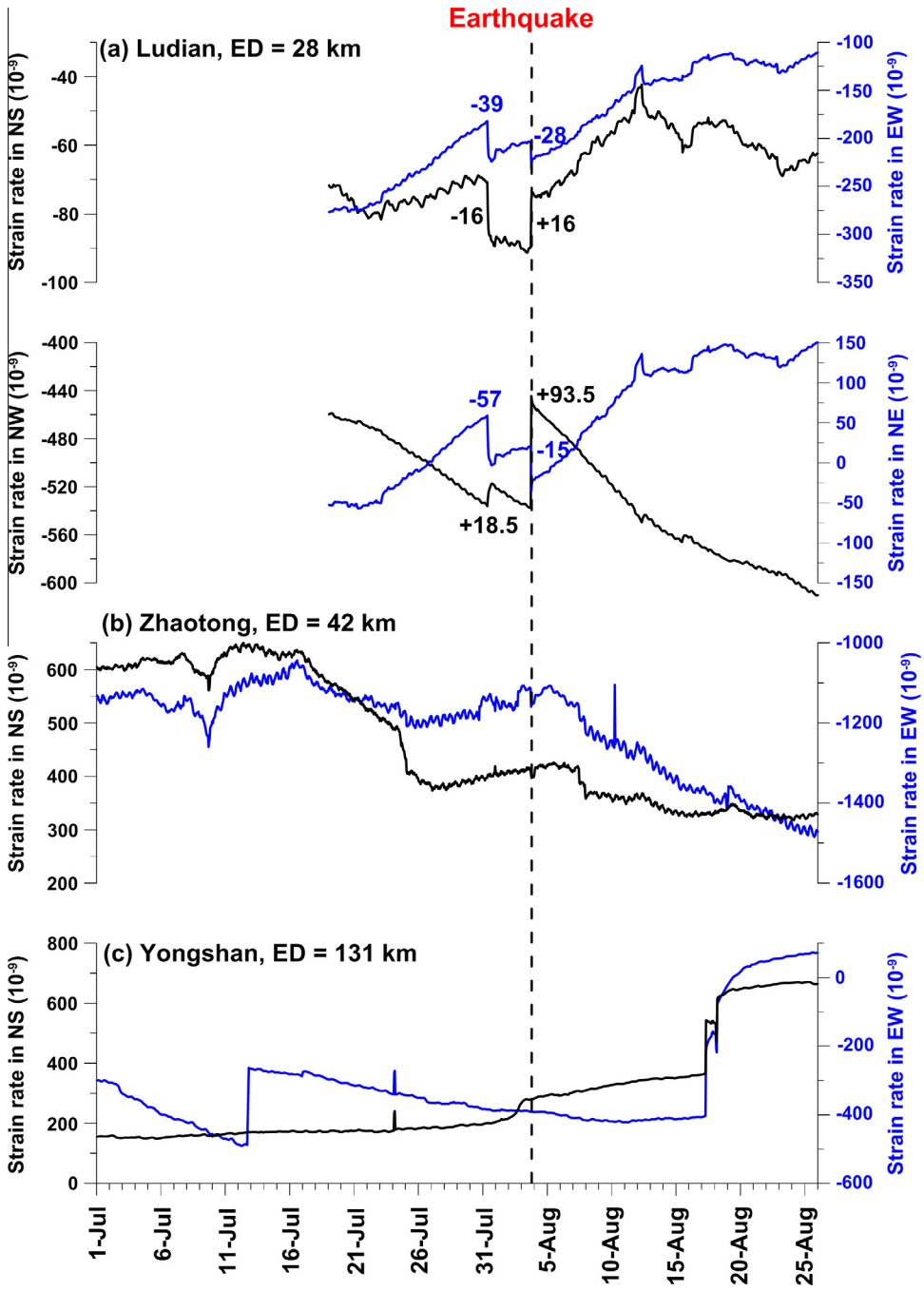

Fig. 3. Variations of strain rates in Ludian, Zhaotong and Yongshan during July 1–August 25. The vertical dash line shows occurrence time of the Ludian earthquake. The numbers are the amplitude of the rapid changes in associated components in Ludian on July 31 and August 3. The data and the accordingly *Y* axis is paired by the same color. ED is the abbreviation of epicentral distance. (For interpretation of the references to color in this figure legend, the reader is referred to the web version of this article.)

different from the other smooth uplifts, was observed on August 1. The unusual sudden change is rarely detected from long-term time-series data and is considered to be the candidate of seismo-water level anomalies associated with the Ludian earthquake. Changes in groundwater levels retrieved from the Qiaojia area are examined and shown in Fig. 2b. A relationship of uplifts and depressions of groundwater levels associated with precipitations can be repeatedly obtained in the Qiaojia area. It is worth mentioning that water temperature and groundwater levels often yield an inversely proportional relationship because precipitations infuse groundwater decreasing the temperature, except for the step-like changes on July 31 that are in-phase at two parameters regardless latter decrease of water temperature. The uplifts of groundwater levels should be dominated by possible mechanisms except for rainfalls because no significant precipitation can be found from the data recorded in Qiaojia on July 31. On the other hand, concentration of the water radon generally maintained at a low stage of about 400 Bq/L during the study period. A box-like change could be found from the variations of the concentration during July 16–25, 2014. In contrast, a depression appeared on approximately July 30, 2014 that is very close to the unusual step-like changes on July in timing. Subsequently, an anomalous drop of the radon concentration occurred from July 31 to August 2 that is related to the sudden uplift of groundwater levels in the

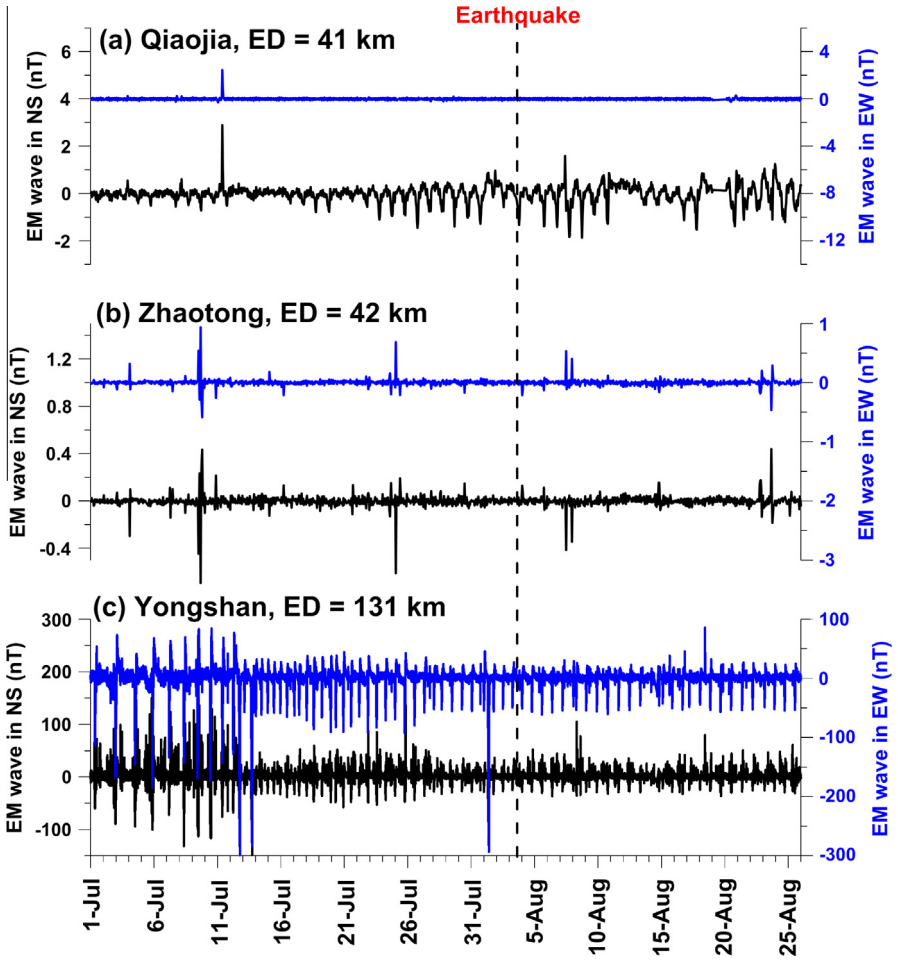

Fig. 4. Changes in electromagnetic field via the EM detector in Qiaojia, Zhaotong and Yongshan during July 1–August 25. The vertical dash line shows occurrence time of the Ludian earthquake. The data and the accordingly *Y* axis is paired by the same color. ED is the abbreviation of epicentral distance. (For interpretation of the references to color in this figure legend, the reader is referred to the web version of this article.)

temporal domain (Fig. 2c). Regarding observations in the Daguan area about 92 km away from the epicenter, uplifts of groundwater levels and precipitations also yield good agreement (Fig. 2d). However, the water temperature in Daguan is rather noisy and is relative insensitivity to groundwater level than it in Qiaojia. The water temperature persistently maintains about 20.82 °C during the study period, except for fluctuation with ±0.01 °C from July 26 to August 3. The fluctuation reached to the maximum on July 28 and rapidly dropped to the minimum on August 1.

3. Observations of strain and electromagnetic field

Strainmeters with a high resolution of about 10^{-9} in the strain rate were installed in Ludian, Zhaotong and Yongshan to monitor strain changes before earthquakes. Variations of the strain rate in the NS, EW, NW and NE components, which are simultaneously recorded by the strainmeter installed in Ludian during the study period, are shown in Fig. 3a. Two significant step-like changes can be found from the strain data on the entire axes, simultaneously, on July 31 and August 3. It is clear that the step-like changes on August 3 would be related to the co-seismic effects associated with the Ludian earthquake. However, causal mechanisms with respect to the step-like changes on July 31 are obscurity when those strain data are solo taken into consideration. Regarding the strain rate recorded in Zhaotong, three significant turning points can be found on the NS and EW components July 1, July 26 and August 9, 2014 (Fig. 3b). The decreasing trend became smooth on July 26 that would suggest the accumulating stress in the crust either approaching the threshold of the fault rupture or becoming mitigation. The transformation (on July 26) of the threshold approach would be an agreement with processes of the seismo-deformation anomalies observed in the previous studies (Chen et al., 2011, 2013a, 2014) while the others (i.e. on July 1 and August 1) were caused by unknown mechanisms. It is clear that the strain rate on the NS and EW components generally showed in-phase changes regardless unknown factors. The discrepancy of changes in the strain rate isolated on the EW axis appeared on July 30 and August 3. Similarly, the changes on August 3 would be affected by co-seismic effects of the Ludian earthquake. In contrast, the changes on July 30, which agrees with the variations of the anomalous strain rate observed in Ludian in timing, are related with indistinct factors. Peaks and step-like changes can be found from the strain rates both on the NS and EW axes on July 12, July 24 an August 18 in Yongshan, where is about 131 km away from the epicenter (Fig. 3c). Those changes are different with the aforementioned anomalies in timing owing to unknown reason and were further eliminated in following discussion. Notably, abnormal changes of gradually increase during July 31–August 3 and mitigation of decrease trend July 27–August 5 can be found on the NS and EW axes, respectively.

EM wave detectors, which monitor changes in the geomagnetic field at the frequency ranged between 0.01 Hz and 20 Hz through induction-coils with a sampling interval of 1 min, were installed

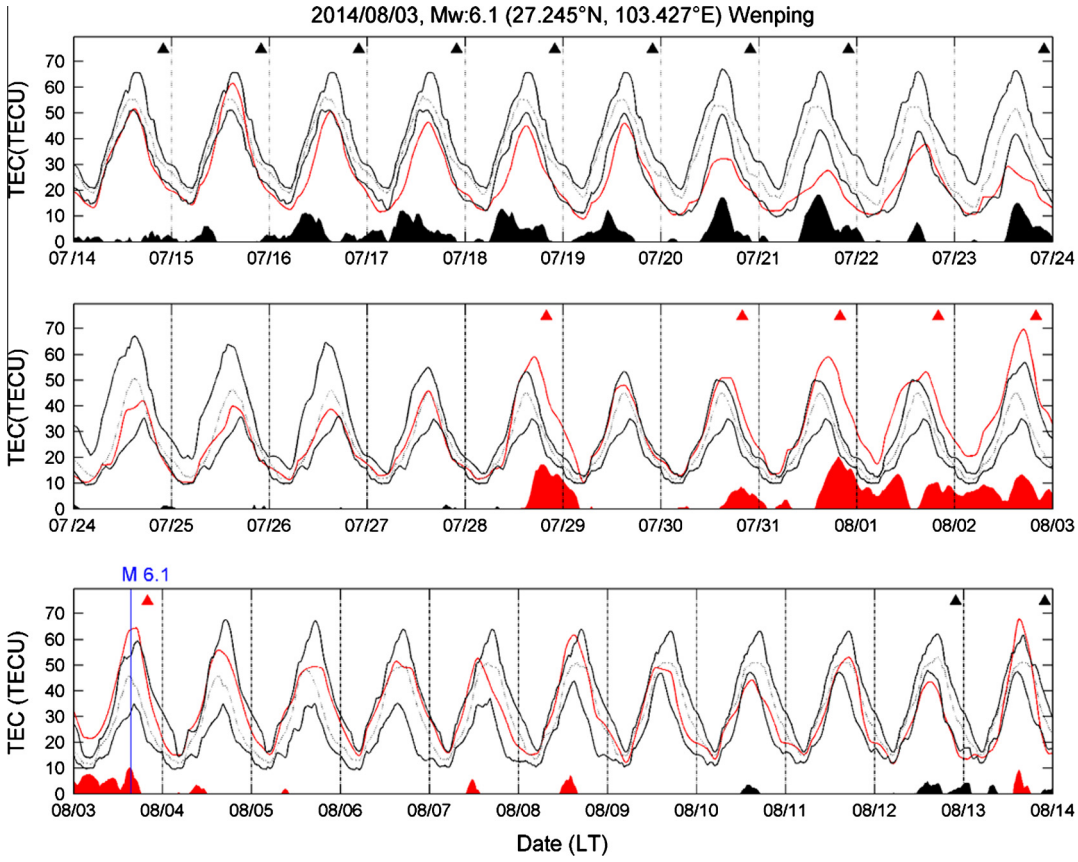

Fig. 5. The temporal distributions of GIM TEC above the 2014 M6.1 Ludian earthquake epicenter from July 14 to August 14, 2014. At each time point, the median, the first (or lower) and the third (or upper) quartiles denoted by *M* (dashed line), *LQ* and *UQ*, respectively, of every successive 15 days of GIM TECs are computed. To have a stringent criterion, the lower and upper bounds are computed via the formulas of $LB = M - 1.5(M–LQ)$ and $UB = M + 1.5(UQ–M)$, respectively, and shown by black lines. The median together with the associated *LB* and *UB* then provide references for the GIM TEC variations on the 16th day. The positive or negative anomalous day are determined and marked by red and black triangles, respectively, once more than one third (=4/12) of the upper or lower abnormal signals (i.e. GIM TEC is greater or smaller than the associated *UB* or *LB*) appear in one day. Note that there are 12 data points per day. (For interpretation of the references to color in this figure legend, the reader is referred to the web version of this article.)

in Qiaojia, Zhaotong and Yougshan with the epicentral distance of about 41 km, 42 km and 131 km surrounding the epicenter, respectively (also see Figs. 1 and 4). Fig. 4 shows hourly variations of the EM waves by using the smooth method at entire stations. The backgrounds of the electromagnetic data in the NS and EW components in Qiaojia both approach 0 nT (Fig. 4a). Amplitudes of fluctuations in the EW component of the electromagnetic field are rather small during the study period, except for a peak on July 11. In contrast, variations of the electromagnetic data in the NS component were ranged between about −2 and 3 nT and became large lying on the background. An indistinct drift of the baseline appeared during July 26–31 and maintained for a long time and mitigated on August 27 (also see the website on http://www.eqzt.com/). A long duration of the abnormal variation from July 26 to August 27 and a short time spin of 3–4 days of aforementioned pre-earthquake phenomena yield discrepancy. Fluctuations of electromagnetic data were relatively small in Zhaotong except for appearance of several peaks and drops (Fig. 4b). It is interesting that an inverse relationship between the data in the NS and EW components can be obtained once those peaks and drops are examined. This suggests that interference was frequently coming from an unknown source at the either NW or SE direction. No significant anomalous phenomena can be found a few days before the Ludian earthquake without further analyses. Electromagnetic data recorded in Yongshan were very noisy because an electric power plant located about 3 km away from the station was operated recently (Fig. 4c). It is very difficult to retrieve useful information from noisy data without removal of the interference from the electric power plant.

4. TEC anomalies in the ionosphere

Fig. 5 shows changes in TEC over the epicenter isolated from GIM between 20 days before and 10 days after the earthquake. To detect abnormal signals of the TEC variations, the standard method of a quartile-based process proposed in the previous study (Liu et al., 2011) is performed. Negative anomalies occurred during July 14–24, except on July 23, while positive anomalies appeared on July 28 and July 31 to August 2 (day 6 and 3–1 before the earthquake). There are 4 positive anomaly days before the earthquake, which are most likely the earthquake related. Notably, the Dst (disturbance storm time) index was ranged from −26 nT to 11 nT from August 1 to August 4 that is rather stable and would not the major factor of the retrieved positive anomalies. To see if the anomalies specifically appeared around the earthquake, a global examination on the GIM TEC would be required. Since the process and areas of the earthquake preparation are generally long and huge, the associated duration of seismo-ionospheric precursors is most likely long. Here, we examine the 90% and greater of the GIM TEC in pervious 1–30 days at each time point during the 4 positive anomaly days. Fig. 6 illustrates that the spatial distributions of 90+% GIM TEC (i.e. the positive anomalies) on July 31, 2014. It can be seen

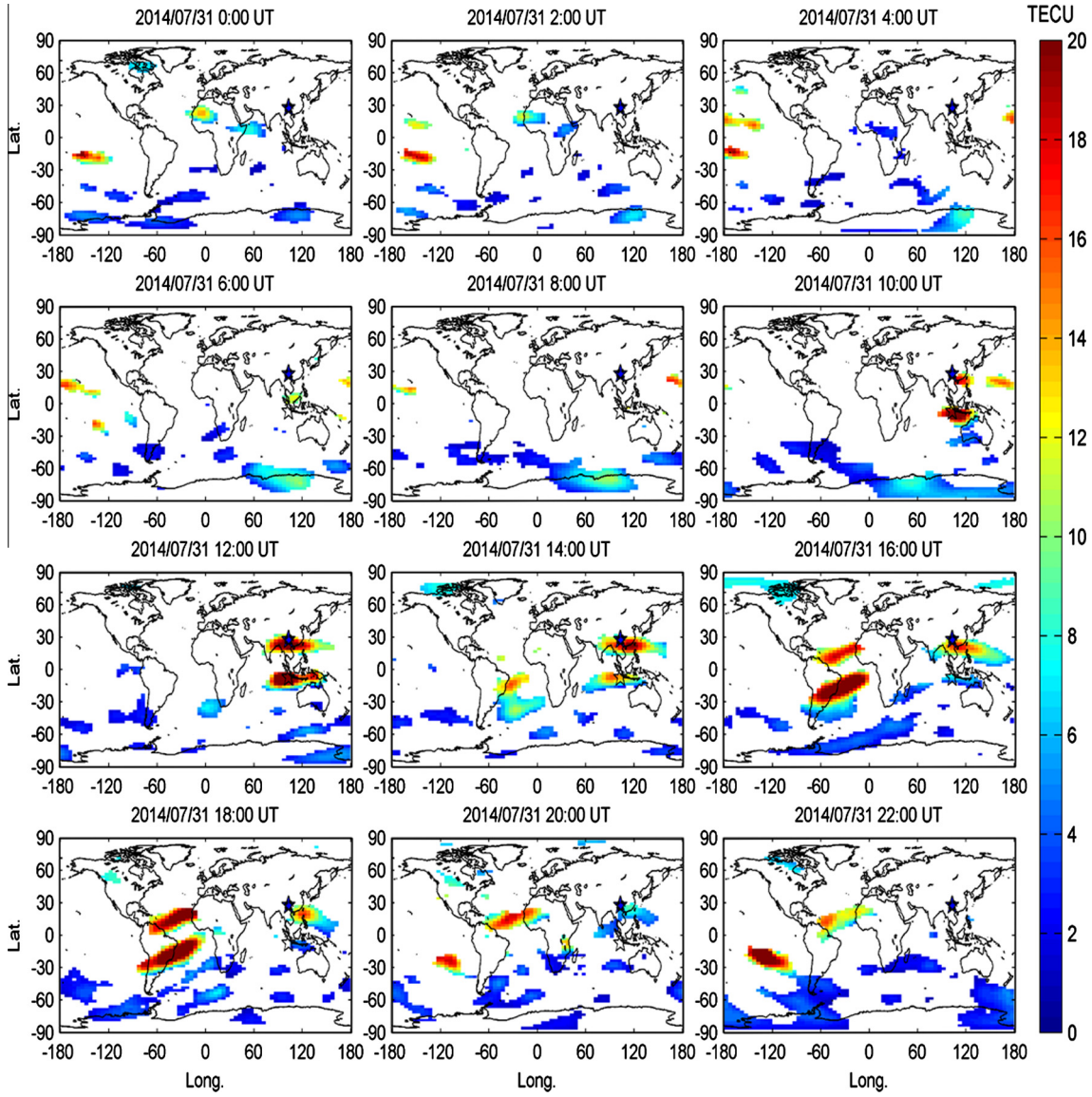

Fig. 6. The GIM TEC anomaly maps on July 31. The GIM TEC with 2-h time resolution covering ±87.5°N latitude and ±180°E longitude ranges with spatial resolutions of 2.5° and 5°, respectively. Each map consists of 5183 (=71 × 73) grid points (or lattices).

that the positive anomalies constantly appear around the epicenter and its conjugate point at 6 time points between 1000 and 2000 UT. Fig. 7 is the superimposed result of the 6-time-point which shows that specifically appear around the epicenter and its southeast area. The anomalous area (20 lattices) seems to be large, and however in comparing to the globe (5183 lattices), the positive anomalies on July 31 are very likely related to the Ludian earthquake.

5. Discussion and conclusions

Scholz et al. (1973) separated the pre-earthquake anomalous phenomena into three stages. No significant anomalous phenomena can be observed in the stage I of buildup of elastic strain. When cracks are developed and dilatant due to stress accumulation in the crust in the stage II, decrease of seismic *P* velocity, uplift and tilt of ground, radon emission and increases of conductivity could be monitored in place stressed. At the stage III, water would infuse into the fault zone and crustal deformation could become unstable. In contrast, uplift and tilt of ground and emission of radon would maintain at a high stage till occurrence of the main shock. Thus, those different physical parameters would potentially change in the same time and should be taken into consideration together once pre-earthquake anomalous phenomena are studied.

It has been examined that there are many anomalies observed from different data recorded around and/or above the epicenter of the Ludian earthquake. However, those anomalous phenomena are very difficult to be related to the Ludian earthquake once recorded data is solo considered. When those physical parameters utilized in this study are concerned, simultaneously, anomalous changes of them each with an anomalous behavior can be observed on common days from July 31 to August 2, except for electromagnetic waves. The timing of those common days rather approaches the occurrence of the Ludian earthquake. The anomalous behaviors from those different parameters are thus suspected to be the earthquake related. Since stress is considered to be the major factor of earthquakes, their relationships are first exposed from strain data. Here, amplitudes associated with co-seismic effects recorded in the NS, EW, NE, NW components in Ludian (Fig. 3a) are computed to compare with the direction of the most compressive axis (i.e. 294°) of the Ludian earthquake to examine the accuracy of the

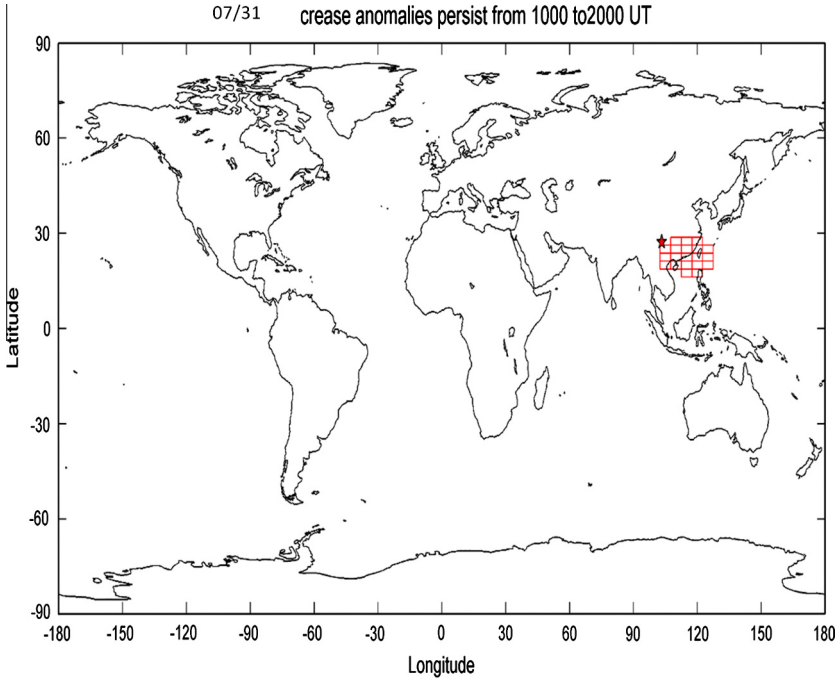

Fig. 7. The superimposed result of the GIM TEC anomaly map obtained on July 31. The red star denotes the location of Ludian earthquake. Meanwhile, areas with red open rectangles are the locations with the persistent positive anomalies determined by using its conjugate point at 6 time points between 1000 and 2000 UT. (For interpretation of the references to color in this figure legend, the reader is referred to the web version of this article.)

strain rate data. The amplitudes are computed by using the turning points at the both ends of the rapid change from strain data on earthquake day. The co-seismic related amplitudes were 1.6×10^{-8}, -2.8×10^{-8}, -1.5×10^{-8} and 9.35×10^{-8} in the NS, EW, NE and NW component, respectively (also see Fig. 3). Directions of the compressive axis derived from the amplitudes in the NS and EW (NE and NW) pair were about 300° (306°) that agrees with the most compressive axis (i.e. about 294°) calculated from the fault plane solution. The agreements suggest that the measurements can fairly reflect modifications of stress. On the other hand, the amplitudes of the rapid changes were -1.6×10^{-8}, -3.9×10^{-8}, -5.7×10^{-8} and 1.85×10^{-8} at the NS, EW, NE and NW directions on July 31, respectively. Directions of the compressive axis were 243° and 247° obtained from two component pairs in Ludian. A certain difference of about 45° between the compressive axis obtained on July 31 and it computed from fault plane solutions suggests accumulation stress in seismogenic processes would be different with released stress during earthquakes for the strike-slip event. A high dense strainmeter array could benefit to understand stress changes in seismogenic processes. Note that the directions of the compressive axis are about 90° and 0° at stations in Zhaotong and Yongshan on July 31 that would relate to the east–west and north–south strikes of the Xiaojiang-Baogunao and Ludian-Zhaotong fracture zones, respectively (Fig. 3b and c).

When loading stress results in strain and modifies permeability of rocks underground, changes in groundwater levels should be observed accordingly. Groundwater levels with a significant increase can be observed in Ludian and Qiaojia on July 29 and August 1 that is consistent with the appearance time of strain changes recorded in Ludian, Zhaotong and Yongshan. Uplift of groundwater levels suggests infusion of groundwater that decreases the water temperature and drops the concentration of radon in Qiaojia on July 29, simultaneously (Fig. 2b and c). Once anomalous increase of water temperature in Daguan is also integrated together, water-related anomalies were found earlier in distance places surrounding and latter in near areas (i.e. about 92, 56 and 28 km away on July 26, July 29 and August 1, respectively). A series of those water-related anomalies also sheds light on exposing a NE–SW tendency of the earthquake-related stress loading. Note that the NE–SW tendency is most likely the direction of the compressive axis obtained from two component pairs in Ludian on July 31. Positive TEC anomalies mainly appeared over the epicenter on July 31 to August 2 (3–1 days before the earthquake) that would resulted from currents due to the activation of positive holes (Freund et al., 2006; Freund, 2010, 2011, 2013), radon release (Pulinets, 2007; Omori et al., 2007; Ouzounov et al., 2011; Sorokin and Hayakawa, 2013) and conductivity changes (Kuo et al., 2011). However, the relationship of the litho sphere–atmosphere–ionosphere coupling regarding the positive TEC anomalies triggered by ground currents and/or radon release is very difficult to be examined at this moment because the major key of the seismo-EM anomalies cannot be clearly indentified in this study without any further analysis.

In short, pre-earthquake anomalies of surface strain, groundwater levels, water temperature, water radon and ionospheric TEC constantly appeared approximately 1–8 days before the Ludain earthquake. Multiple-parameter comparison through potential mechanisms is useful for eliminating anomalies sometimes related to unknown factors and reducing the risk of earthquake forecast by using one isolated parameter. In contrast, no significant anomaly observed from the raw data of EM waves suggests that determination of pre-earthquake phenomena would be dependent on analytical methods, signal and noise ratios and/or different types of earthquakes. Forecast ability of the multiple-parameter comparison will be examined and/or evaluated once more results derived more different-type earthquakes are collected in the near future.

Acknowledgements

The authors wish to express appreciation to Infosystem for Earthquake Disaster Mitigation Bureau of Zhaotong, Yunnan

providing the types of invaluable observation data. This work was supported by Ministry of Science and Technology, Taiwan with Grant Numbers NOST 103-2116-M-194-015-MY3 and MOST 103-2116-M-194-006.

References

Barbot, S., Fialko, Y., 2010. A unified continuum representation of post-seismic relaxation mechanisms: semi-analytic models of afterslip, poroelastic rebound and viscoelastic flow: semi-analytic models of postseismic transient. Geophys. J. Int. 182, 1124–1140.

Barbot, S., Hamiel, Y., Fialko, Y., 2008. Space geodetic investigation of the coseismic and postseismic deformation due to the 2003 Mw7.2 Altai earthquake: implications for the local lithospheric rheology. J. Geophys. Res. 113, B03403.

Bredehoeft, J.D., 1967. Response of well-aquifer systems to Earth tides. J. Geophys. Res. 72, 3075–3087.

Chen, C.H., Liu, J.Y., Yang, W.H., Yen, H.Y., Hattori, K., Lin, C.R., Yeh, Y.H., 2009. SMART analysis of geomagnetic data observed in Taiwan. Phys. Chem. Earth 34, 350–359. http://dx.doi.org/10.1016/j.pce.2008.09.002.

Chen, C.H., Liu, J.Y., Lin, P.Y., Liang, W.T., Yen, H.Y., Hattori, K., Zeng, X., 2010. Pre-seismic geomagnetic anomaly and earthquake location. Tectonophysics 489, 240–247. http://dx.doi.org/10.1016/j.tecto.2010.04.018.

Chen, C.H., Yeh, T.K., Liu, J.Y., Wang, C.H., Wen, S., Yen, H.Y., Chang, S.H., 2011. Surface deformation and seismic rebound: implications and applications. Surv. Geophys. 32, 291–313. http://dx.doi.org/10.1007/s10712-011-9117-3.

Chen, C.H., Wen, S., Yeh, T.K., Wang, C.H., Yen, H.Y., Liu, J.Y., Hobara, Y., Han, P., 2013a. Observation of surface displacements from GPS analyses before and after the Jiashian earthquake (M = 6.4) in Taiwan. J. Asian Earth Sci. 62, 662–671. http://dx.doi.org/10.1016/j.jseaes.2012.11.016.

Chen, C.H., Wang, C.H., Wen, S., Yeh, T.K., Lin, C.H., Liu, J.Y., Yen, H.Y., Lin, C., Rau, R.J., Lin, T.W., 2013b. Anomalous frequency characteristics of groundwater level before major earthquake in Taiwan. Hydrol. Earth Syst. Sci. 17, 1693–1703. http://dx.doi.org/10.5194/hess-17-1693-2013.

Chen, C.H., Hsu, H.L., Wen, S., Yeh, T.K., Chang, F.Y., Wang, C.H., Liu, J.Y., Sun, Y.Y., Hattori, K., Yen, H.Y., Han, P., 2013c. Evaluation of seismo-electric anomalies using magnetic data in Taiwan. Nat Hazards Earth Syst Sci 13, 597–604. http://dx.doi.org/10.5194/nhess-13-597-2013.

Chen, C.H., Wen, S., Liu, J.Y., Hattori, K., Han, P., Hobara, Y., Wang, C.H., Yeh, T.K., Yen, H.Y., 2014. Surface displacements in Japan before the 11 March 2011 M9.0 Tohoku-Oki earthquake. J. Asian Earth Sci. 80, 165–171. http://dx.doi.org/10.1016/j.jseaes.2012.11.016.

Chen, C.H., Tang, C.C., Cheng, K.C., Wang, C.H., Wen, S., Lin, C.H., Wen, Y.Y., Meng, G., Yeh, T.K., Jan, J.C., Yen, H.Y., Liu, J.Y., 2015. Groundwater-strain coupling before the 1999 Mw 7.6 Taiwan Chi-Chi earthquake. J. Hydrol. 524, 378–384. http://dx.doi.org/10.1016/j.jhydrol.2015.03.006.

Chia, Y., Wang, Y.S., Chiu, J.J., Liu, C.W., 2001. Changes of groundwater level due to the 1999 Chi–Chi earthquake in the Choshui River Alluvial Fan in Taiwan. Bull. Seismol. Soc. Am. 91, 1062–1068.

Fenoglio, M.A., Johnston, M.J.S., Byerlee, J.D., 1995. Magnetic and electric fields associated with changes in high pore pressure in fault zone-application to the Loma Prieta ULF emissions. J. Geophys. Res. 100, 12951–12958.

Fraser-Smith, A.C., Bernardi, A., McGill, P.R., Ladd, M.E., Helliwell, R.A., Villard Jr., O.G., 1990. Low-frequency magnetic field measurements near the epicenter of the Ms 7.1 Loma Prieta earthquake. Geophys. Res. Lett. 17, 1465–1468.

Freund, F., 2010. Toward a unified solid state theory for pre-earthquake signals. Acta Geophys. 58, 719–766.

Freund, F., 2011. Pre-earthquake signals: underlying physical processes. J. Asian Earth Sci. 41, 383–400.

Freund, F., 2013. Earthquake forewarning – a multidisciplinary challenge from the ground up to space. Acta Geophys. 61, 775–807.

Freund, F., Takeuchi, A., Lau, B.W., 2006. Electric currents streaming out of stressed igneous rocks – A step towards understanding pre-earthquake low frequency EM emissions. Phys. Chem. Earth 31, 4–9.

Ghosh, D., Deb, A., Sengupta, R., 2009. Anomalous radon emission as precursor of earthquake. J. Appl. Geophys. 69, 67–81.

Han, P., Huang, Q., Xiu, J., 2009. Principal component analysis of geomagnetic diurnal variation associated with earthquakes: case study of the M6.1 Iwate-ken Nairiku Hokubu earthquake. Chinese J. Geophys. 52, 1556–1563. http://dx.doi.org/10.3969/j.issn.0001-5733.2009.06.017.

Han, P., Hattori, K., Huang, Q., Hirano, T., Ishiguro, Y., Febriani, F., Yoshino, C., 2011. Evaluation of ULF electromagnetic phenomena associated with the 2000 Izu Islands earthquake swarm by wavelet transform analysis. Nat Hazards Earth Syst Sci 11, 965–970. http://dx.doi.org/10.5194/nhess-11-965-2011.

Han, P., Hattori, H., Hirokawa, M., Zhuang, J., Chen, C.H., Febriani, F., Yamaguchi, H., Yoshino, C., Liu, J.Y., Yoshida, S., 2014. Statistical analysis of ULF seismo-magnetic phenomena at Kakioka, Japan, during 2001–2010. J. Geophys. Res. 119, 4998–5011.

Han, P., Hattori, K., Xu, G., Ashida, R., Chen, C.H., Febriani, F., Yamaguchi, H., 2015. Further investigations of geomagnetic diurnal variations associated with the 2011 off the Pacific coast of Tohoku earthquake (Mw9.0). J. Asian Earth Sci. 114, 321–326.

Hattori, K., 2004. ULF geomagnetic changes associated with large earthquakes. Terr. Atmos. Ocean. Sci. 15, 329–360.

Hattori, K., Han, P., Yoshino, C., Febriani, F., Yamaguchi, H., Chen, C.H., 2013. Investigation of ULF seismo-magnetic phenomena in Kanto, Japan during 2000–2010: case studies and statistical studies. Surv. Geophys. 34, 293–316. http://dx.doi.org/10.1007/s10712-012-9215-x.

Huang, Q., 2002. One possible generation mechanism of co-seismic electric signals. Proc. Jpn. Acad. Ser. B 78, 173–178.

Kingsley, S.P., Biagi, P.E., Piccolo, R., Capozzi, V., Ermini, A., Khatkevich, Y.M., Gordeev, E.I., 2001. Hydrogeochemical precursors of strong earthquakes: a realistic possibility in Kamchatka. Phys. Chem. Earth 26, 769–774.

Kuo, T., Fan, K., Kuochen, H., Han, Y., Chu, H., Lee, Y., 2006. Anomalous decrease in groundwater radon before the Taiwan M = 6.8 Chengkung earthquake. J. Environ. Radioact. 88, 101–106.

Kuo, C.L., Huba, J.D., Joyce, G., Lee, L.C., 2011. Ionosphere plasma bubbles and density variations induced by pre-earthquake rock currents and associated surface charges. J. Geophys. Res. 116 (A10317), 2011.

Lin, Y., Zeng, X., 1992. The response of anomalous short period geomagnetic variations to moderate-strong earthquakes in China. J. Earthquake Prediction Res. 8, 1–10.

Liu, J.Y., Chen, C.H., Chen, Y.I., Yen, H.Y., Hattori, K., Yumoto, K., 2006. Seismo-geomagnetic anomalies and M > 5.0 earthquakes observed in Taiwan during 1988–2001. Phys. Chem. Earth 30, 215–222.

Liu, J.Y., Chen, Y.I., Chen, C.H., Liu, C.Y., Chen, C.Y., Nishihashi, M., Li, J.Z., Xia, Y.Q., Oyama, K.-I., Hattori, K., Lin, C.H., 2009. Seismo-ionospheric GPSTEC anomalies observed before the 12 May 2008 Mw7.9 Wenchuan earthquake. J. Geophys. Res. 114, A04320. http://dx.doi.org/10.1029/2008JA013698.

Liu, J.Y., Chen, Y.I., Chen, C.H., Hattori, K., 2010. Temporal and spatial precursors in the ionospheric global positioning system (GPS) total electron content observed before the 26 December 2004 M9.3 Sumatra-Andaman earthquake. J. Geophys. Res. 115 (A09312), 2010J. http://dx.doi.org/10.1029/A015313.

Liu, J.Y., Le, H., Chen, Y.I., Chen, C.H., Liu, L., Wan, W., Su, Y.Z., Sun, Y.Y., Lin, C.H., Chen, M.Q., 2011. Observations and simulations of seismoionospheric GPS total electron content anomalies before the 12 January 2010 M7 Haiti earthquake. J. Geophys. Res. 116, A04302. http://dx.doi.org/10.1029/2010JA015704.

Merzer, M., Klemperer, S.L., 1997. Modeling low-frequency magnetic-field precursor to the Loma Prieta earthquake with a precursory increase in fulat-zone conductivity. Pure Appl. Geophys. 150, 217–248.

Molchanov, O.A., Hayakawa, M., 1995. Generation of ULF electromagnetic emissions by microfracturing. Geophys. Res. Lett. 22, 3091–3094.

Molchanov, O.A., Hayakawa, M., 2008. Seismo Electromagnetics and Related Phenomena: History and Latest Results. Terra Scientific, Pub. Comp., Tokyo, pp. 189.

Nagata, T., 1970. Anisotropic magnetic susceptibility of rocks under mechanical stresses. Pure Appl. Geophys. 78, 110–122.

Omori, Y., Yasuoka, Y., Nagahama, H., Kawada, Y., Ishikawa, T., Tokonami, S., Shinagi, M., 2007. Anomalous radon emanation linked to preseismic electromagnetic phenomena. Nat. Hazards Earth Syst. Sci. 7, 629–635. http://dx.doi.org/10.5194/nhess-7-629-2007.

Ouzounov, D., Pulinets, S., Romanov, A., Alexander, R., Konstantin, T., Dmitri, D., Menas, K., Patrick, T., 2011. Atmosphere–Ionosphere response to the M9 Tohoku earthquake revealed by joined satellite and ground observations: preliminary results. Earthquake Sci. 24, 557–564.

Peltzer, G., Rosen, P., Rogez, F., Hudnut, K., 1998. Poroelastic rebound along the Landers 1992 earthquake surface rupture. J. Geophys. Res. 103 (B12), 30131–30145. http://dx.doi.org/10.1029/98JB02302.

Pulinets, S.A., 2007. Natural radioactivity, earthquakes, and the ionosphere. EOS Trans. Am. Geophys. Union 88, 217–218.

Quilty, E.G., Roeloffs, E.A., 1997. Water level changes in response to the December 20, 1994 M4.7 earthquake near Parkfield, California. Bull. Seismol. Soc. Am. 87, 310–317.

Robinson, R., McGinty, P.J., 2000. The enigma of the Arthur's Pass, New Zealand, earthquake 2. The aftershock distribution and its relation to regional and induced stress field. J. Geophys. Res. 105, 16139–16150.

Roeloffs, E.A., 1988. Hydrologic precursors to earthquakes: a review. Pure Appl. Geophys. 126, 177–206.

Roeloffs, E.A., 1998. Persistent water level changes in a well near Parkfield, California, due to local and distant earthquakes. J. Geophys. Res. 93, 13619–13634.

Scholz, C.H., Sykes, L.R., Aggarwal, Y.P., 1973. Earthquake prediction: a physical basis. Science 181, 803–810.

Smith, E.F., Gomberg, J., 2009. A search in strainmeter data for slow slip associated with triggered and ambient tremor near Parkfield, California. J. Geophys. Res. 114, B00A14. http://dx.doi.org/10.1029/2008JB006040.

Sorokin, V., Hayakawa, M., 2013. Generation of seismic-related DC electric fields and lithosphere–atmosphere–ionosphere coupling. Modern Appl. Sci. 7, 1–25.

Stacey, F.D., 1962. Theory of the magnetic susceptibility of stressed rocks. Phil. Mag. 7, 551–556.

Wakita, H., Nakamura, Y., Notsu, K., Noguchi, M., Asada, T., 1980. Radon anomaly-possible precursor of the 1978 Izu-Oshima-Kinkai earthquake. Science 207, 882–883.

Wang, C.-Y., Cheng, L.H., Chin, C.V., Yu, S.B., 2001. Coseismic hydrologic response of an alluvial fan to the 1999 Chi–Chi earthquake, Taiwan. Geology 29, 831–834.

Wen, S., Chen, C.H., Yen, H.Y., Yeh, T.K., Liu, J.Y., Katsumi, K., Han, P., Wang, C.H., Shin, T.C., 2012. Magnetic storm free ULF analysis in relation with earthquakes in Taiwan. Nat. Hazards Earth Syst. Sci. 12 (1747–1754), 2012. http://dx.doi.org/10.5194/nhess-12-1747-2012.

Xu, G., Han, P., Huang, Q., Hattori, K., Febriani, F., Yamaguchi, H., 2013. Anomalous behaviors of geomagnetic diurnal variations prior to the 2011 off the Pacific coast of Tohoku earthquake (M_w9.0). J. Asian Earth Sci. 77, 59–65.

Yen, H.Y., Chen, C.H., Yeh, Y.H., Liu, J.Y., Lin, C.R., Tasi, Y.B., 2004. Geomagnetic fluctuations during the 1999 Chi–Chi earthquake in Taiwan. Earth Planets Space 56, 39–45.

Zeng, X., Lin, Y., Zhu, Z., Xu, R., Zhao, M., Zhang, C., Liu, Q., 1995. Study on electric variations of media in epicentral area by geomagnetic transfer functions. Acra Seismologica Sinica 1, 413–418.